Inviscid flow of a reacting mixture of gases around a blunt body

By WILBERT LICK
Pierce Hall, Harvard University, Cambridge, Mass.

(Received 13 April 1959)

A general numerical procedure is described whereby the details of the steady inviscid flow of a mixture of perfect gases about a blunt body, including the effects of finite dissociation and recombination rates, may be calculated. Several numerical examples are calculated in order to apply the numerical procedure to specific cases and also to show the effects of finite reaction times on the flow about a blunt body.

1. Introduction

A considerable amount of effort has been expended recently on the problem of predicting the flow about a blunt body, particularly at high speeds. Almost all of the published papers on this problem have dealt with flow in chemical equilibrium. However, at hypersonic speeds and therefore with high temperatures near the body, the assumption of equilibrium flow becomes questionable. Recent studies (Gunn 1952; Logan 1957; Freeman 1957) have indicated that finite reaction times may have an appreciable effect on the flow properties. A detailed analysis of the non-equilibrium flow is necessary to predict the flow field accurately.

After presenting the fundamental equations and boundary conditions for the inviscid non-heat-conducting flow of a mixture of perfect gases, the present paper describes an inverse method whereby, if the form of the detached shock wave is known or is assumed, the field behind the shock and the corresponding shape of the body may be found. For the continuation of the solution in the supersonic region, a method of characteristics is presented. In order to perform numerical computations, a rough analysis of dissociation and recombination rates is made. The results of several numerical calculations are then presented.

Although the theory and numerical procedure can be easily extended to include finite reaction times for rotation, vibration and ionization, the assumption is made that the rotational and vibrational degrees of freedom are in equilibrium with the translational degrees of freedom, while ionization is neglected. The rate of change of the various components of the gas mixture towards their equilibrium distribution, i.e. towards local thermodynamic equilibrium of the complete system, is governed by dissociation and recombination rate equations. Diffusion of the gases is neglected.

2. Fundamental equations and boundary conditions

For each of the n components of the gas, the equation of state is

$$p_i = \rho_i \frac{R}{M_i} T,$$

where p_i denotes the pressure, ρ_i the density, and M_i the molecular weight of the ith component of the gas. The equation of state for a mixture of perfect gases is obtained by summation and is

$$p = \rho \frac{R}{M} T, \tag{1}$$

where

$$\frac{1}{M} = \sum_i \frac{\rho_i}{\rho} \frac{1}{M_i}.$$

The conservation equations for a gas mixture have been given by Hirschfelder, Curtiss & Bird (1954), Penner (1955), and others. They are presented here in the most convenient form for the present analysis subject to the previous approximations.

For each component of the gas, the continuity equation is

$$\nabla.(\rho_i \mathbf{V}) = \omega_i, \tag{2}$$

where $\mathbf{V}$ is velocity, and ω_i represents the mass rate of production of the component by chemical reaction. By summation over all components of the gas, the overall continuity equation is obtained

$$\nabla.(\rho \mathbf{V}) = 0. \tag{3}$$

By use of the above equation, (2) can be rewritten in the form

$$\frac{D\alpha_i}{Dt} = (\mathbf{V}.\nabla)\,\alpha_i = \frac{\omega_i}{\rho}, \tag{4}$$

where $\alpha_i = \rho_i/\rho$.

The momentum equation is simply

$$\rho(\mathbf{V}.\nabla)\,\mathbf{V} + \nabla p = 0. \tag{5}$$

The energy equation is

$$d(h + \tfrac{1}{2}\mathbf{V}^2) = 0, \tag{6}$$

where $h = \sum_i \alpha_i h_i$, and h_i is the enthalpy of each component of the gas, which can be separated into energies due to the active degrees of freedom (translational, rotational and vibrational), the energy of dissociation, and a term p_i/ρ_i: thus

$$h_i = E_{ai} + E_{Di} + \frac{p_i}{\rho_i}.$$

The enthalpy of each component of the gas depends only on the temperature and can be calculated from the equations

$$E_{ai} + \frac{p_i}{\rho_i} = \beta_i \frac{R}{M_i} T,$$

$$E_{Di} = \frac{D_i}{2M_i}.$$

The β's are known functions of the temperature, while the dissociation energy D is a constant. By use of the above relations, the energy equation can be written in the two equivalent forms

$$\sum_i \alpha_i \beta_i \frac{R}{M_i} dT + \sum_i \alpha_i \frac{R}{M_i} T\, d\beta_i + \sum_i h_i\, d\alpha_i + d(\tfrac{1}{2}\mathbf{V}^2) = 0, \tag{7a}$$

$$c_{p_a} dT + \sum_i h_i\, d\alpha_i + d(\tfrac{1}{2}\mathbf{V}^2) = 0, \tag{7b}$$

where $c_{p_a} = \sum_i \alpha_i c_{p_{ai}}$.

It is assumed that, at a wall, the gas does not interact chemically with the wall, i.e. the wall is non-catalytic. At the solid boundary, the velocity component normal to the wall must be zero; the tangential component is not subject to constraint since the fluid is inviscid.

The boundary conditions at a shock wave can be simplified by resolving the free-stream velocity into components normal and tangential to the shock. The shock transition can then be regarded from a local co-ordinate system moving with a speed equal to the tangential component of velocity. If all the vibrational relaxation distances are very short in comparison with dissociation relaxation distances and in comparison with a typical body dimension, then the properties of the gas immediately after the vibrational degrees of freedom have come to equilibrium and before dissociation has begun may be found by treating the flow by one-dimensional analysis.

The continuity, momentum, and energy equations for one-dimensional flow through a normal shock are, in a usual notation,

$$\rho_\infty v_\infty = \rho_s v_s = c_1, \tag{8}$$

$$p_\infty + \rho_\infty v_\infty^2 = p_s + \rho_s v_s^2 = c_2, \tag{9}$$

$$h_\infty + \tfrac{1}{2} v_\infty^2 = h_s + \tfrac{1}{2} v_s^2 = c_3, \tag{10}$$

where the subscript ∞ refers to free stream conditions in front of the shock and the subscript s refers to conditions immediately behind the shock. Since it is assumed that dissociation has not begun, the enthalpy immediately behind the shock can be written as

$$h_s = \bar{\beta}_s \frac{p_s}{s}, \quad \text{where} \quad \bar{\beta} = \sum_i \alpha_i \frac{M}{M_i} \beta_i.$$

The normal-shock equations plus the equation of state must be solved by an iteration procedure because of the dependence of the β_i's on the temperature and the resulting algebraic complexity of the equations. To accomplish this, the density ρ_s can be found as a function of the temperature, and v_s, p_s, and T_s can be found in terms of ρ_s: thus

$$\rho_s = \frac{\bar{\beta}_s c_2 + \sqrt{\{(\bar{\beta}_s c_2)^2 - 4c_1^2 c_3(\bar{\beta}_s - \tfrac{1}{2})\}}}{2c_3}, \tag{11}$$

$$v_s = \frac{c_1}{\rho_s}, \tag{12}$$

$$p_s = c_2 - \frac{c_1^2}{\rho_s}, \tag{13}$$

$$T_s = \frac{p_s}{\rho_s} \frac{M_s}{R}. \tag{14}$$

Once the free stream conditions are known, c_1, c_2, and c_3 can be calculated. By assuming T_s, β_s can be calculated and equations (11) to (14) can be solved in succession. The process is continued until the assumed T_s and the T_s calculated from (14) agree to the desired accuracy.

3. Inverse method of axisymmetric flow

The inverse method of finding the body shape and the flow field behind a detached shock when the form of the shock wave is given has been successfully applied by other investigators (Zlotnick & Newman 1957; Van Dyke 1958) to the blunt body problem with the restrictions of equilibrium flow, a perfect gas, and constant specific heats. Although the inverse problem as presented here and by the above authors is a Cauchy problem for elliptic equations and is therefore improperly given, it has been shown that accurate solutions may be found by this method if proper care is taken.

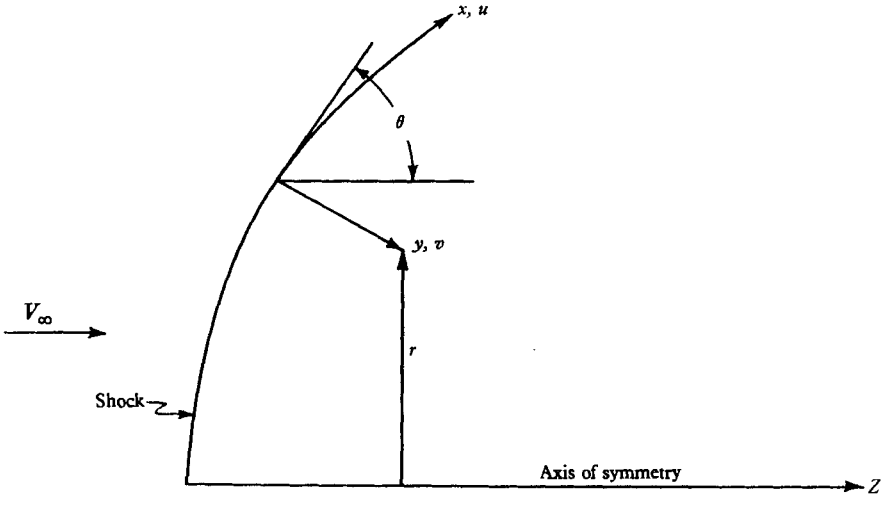

FIGURE 1. Co-ordinate system. Shock radius of curvature at $x = 0$ is R_0.

To simplify the analysis, it is advantageous to choose a natural co-ordinate system which contains the shock wave as one of its surfaces, is applicable to a wide range of shock shapes, and is not restricted to a particular family of curves. Such an orthogonal curvilinear co-ordinate system is shown in figure 1. The origin of the co-ordinate system is taken at the intersection of the shock and the axis of symmetry. Let x be the distance along the shock surface, and let y be the co-ordinate normal to the shock surface. Let u and v be respectively the velocities in the x- and y-directions. Let

$$K = \frac{d\theta}{dx} = -\frac{1}{R},$$

where K is a known function of x for a given shock shape. The local shock radius of curvature is R, and θ is the local angle which the shock makes with the free stream.

The equations of motion, written in the above co-ordinate system, are

$$\frac{u}{1+Ky}\frac{\partial \alpha_i}{\partial x}+v\frac{\partial \alpha_i}{\partial y}=\frac{\omega_i}{\rho}, \tag{15}$$

$$\frac{\partial}{\partial x}[\rho ur]+\frac{\partial}{\partial y}[\rho vr(1+Ky)]=0, \tag{16}$$

$$u\frac{\partial u}{\partial x}+Kuv+(1+Ky)v\frac{\partial u}{\partial y}=-\frac{1}{\rho}\frac{\partial p}{\partial x}, \tag{17}$$

$$u\frac{\partial v}{\partial x}+(1+Ky)v\frac{\partial v}{\partial y}-Ku^2=-\frac{1+Ky}{\rho}\frac{\partial p}{\partial y}, \tag{18}$$

$$\sum_i \alpha_i\beta_i\frac{R}{M}dT+\sum_i \alpha_i\frac{R}{M_i}Td\beta_i+\sum_i h_i d\alpha_i+d(\tfrac{1}{2}\mathbf{V}^2)=0. \tag{19}$$

The additional relation that is needed is the equation of state

$$p=\rho\frac{R}{M}T, \tag{20}$$

and the reaction rates must also be known.

Algebraic manipulation of the above equations yields the following set of relations for the y-derivatives of α_i, u, v, p, and ρ, where the substitutions

$$K_1=\sum_i \alpha_i\frac{R}{M_i}\beta_i, \quad K_2=\sum_i \alpha_i\frac{R}{M_i}\frac{d\beta_i}{dT}$$

have been made:

$$\frac{\partial \alpha_i}{\partial y}=\frac{1}{v}\left[\frac{\omega_i}{\rho}-\frac{u}{1+Ky}\frac{\partial \alpha_i}{\partial x}\right], \tag{21}$$

$$\frac{\partial u}{\partial y}=\frac{1}{v(1+Ky)}\left[-\frac{1}{\rho}\frac{\partial p}{\partial x}-Kuv-u\frac{\partial u}{\partial x}\right], \tag{22}$$

$$\begin{aligned}\frac{\partial v}{\partial y}\left[\frac{v}{T}+(K_1+K_2T)\left(\frac{1}{v}-\frac{Mv}{RT}\right)\right]&=-\frac{u}{T}\frac{\partial u}{\partial y}-\sum_i\left[\frac{h_i}{T}-(K_1+K_2T)\frac{M}{M_i}\right]\frac{\partial \alpha_i}{\partial y}\\&+\frac{K_1+K_2T}{1+Ky}\left[\frac{M}{RT}\left(u\frac{\partial v}{\partial x}-Ku^2\right)-\frac{1}{v}\left(\frac{\partial u}{\partial x}+\frac{u}{\rho}\frac{\partial \rho}{\partial x}+\frac{u}{r}\frac{\partial r}{\partial x}+vK+(1+Ky)\frac{v}{r}\frac{\partial r}{\partial y}\right)\right],\end{aligned} \tag{23}$$

$$\frac{\partial p}{\partial y}=-\frac{\rho}{1+Ky}\left[u\frac{\partial v}{\partial x}+(1+Ky)v\frac{\partial v}{\partial y}-Ku^2\right], \tag{24}$$

$$\frac{\partial \rho}{\partial y}=-\frac{\rho}{v(1+Ky)}\left[(1+Ky)\frac{\partial v}{\partial y}+\frac{\partial u}{\partial x}+\frac{u}{\rho}\frac{\partial \rho}{\partial x}+(1+Ky)\frac{v}{r}\frac{\partial r}{\partial y}+vK+\frac{u}{r}\frac{\partial r}{\partial x}\right]. \tag{25}$$

The boundary conditions at points at equal intervals along the shock can be found by the procedure described previously. The x-derivatives of all dependent variables can then be easily calculated. Once the dependent variables and their x-derivatives are known along the line y_n = const., the above equations can be solved successively and yield the derivatives in a direction normal to the shock.

The quantities (u, for example) at a station y_{n+1} can then be found, as a first approximation, by linear extrapolation

$$u_{n+1}=u_n+\left(\frac{\partial u}{\partial y}\right)_n\Delta y_{n,n+1},$$

where

$$\Delta y_{n,n+1}=y_{n+1}-y_n.$$

From the equation of state, the temperature is determined. The β_i's, which can be written as simple polynomials dependent on T, can then be calculated. All derivatives of the functions at y_{n+1} are subsequently found in a similar manner. An improved value for the function at y_{n+1} can be evaluated by using the average of the derivatives in the y-direction at stations n and $n+1$ or

$$u_{n+1} = u_n + \frac{\Delta y_{n,n+1}}{2}\left[\left(\frac{\partial u}{\partial y}\right)_n + \left(\frac{\partial u}{\partial y}\right)_{n+1}\right].$$

The iteration procedure is then continued until the desired accuracy is obtained.

The integration proceeds in a direction normal to the shock by applying this method to successive intervals in the y-direction.

The surface of the body is determined by applying a continuity analysis to the flow. The mass flow in the x-direction through the surface $x = x_1$ between the shock and station y_N is

$$\pi\rho_s u_s r_s \Delta y_{0,1} + \pi \sum_1^{N-1} \rho_n u_n r_n (\Delta y_{n-1,n} + \Delta y_{n,n+1}) + \pi\rho_N u_N r_N \Delta y_{N-1,N}.$$

The mass flow through the shock between $x = 0$ and $x = x_1$ is $\pi\rho_\infty V_\infty r_s^2$. The body surface can then be determined by calculating the y-ordinate at which the two mass flows are equated.

4. Method of characteristics

As x increases, the distance from the body to the shock also increases, and a larger number of intervals are required to reach the body by the inverse method causing large errors to develop before the body is reached. A more suitable procedure of extending the solution is by the method of characteristics. The calculations by the inverse method in the supersonic region can also be checked by the method of characteristics. The characteristic equations will be presented for both plane and axisymmetric flows using rectangular Cartesian co-ordinates.

By using the standard techniques, the characteristic equations and directions can be found. The characteristic directions correspond to (1) the streamlines, along which the following characteristic equations apply:

$$u\,dy - v\,dx = 0, \tag{26}$$

$$u\frac{\partial \alpha_i}{\partial x} + v\frac{\partial \alpha_i}{\partial y} = \frac{\omega_i}{\rho}, \tag{27}$$

$$d\left(\frac{V^2}{2}\right) + \frac{1}{\rho}dp = 0, \tag{28}$$

and (2) the Mach lines, along which the following characteristic equations apply:

$$\frac{dy}{dx} = \tan(\theta \pm \alpha), \tag{29}$$

$$\frac{1}{\tan\alpha}\frac{dp}{\rho V^2} \pm d\theta = \frac{a}{V}\delta \pm s\left\{-\frac{\epsilon}{y}\sin\theta - \sum_i \frac{h_i}{V c_{p_a} T}\frac{\omega_i}{\rho} + \sum_i \frac{1}{V}\frac{M}{M_i}\frac{\omega_i}{\rho}\right\}, \tag{30}$$

where α is the angle which the Mach lines make with the streamline, a is the 'frozen' speed of sound defined as

$$a^2 = \left(\frac{\partial p}{\partial \rho}\right)_{s,\alpha_i} = \gamma_a \frac{R}{M} T,$$

where γ_a is the ratio of specific heats of the active degrees of freedom, and θ is the angle of flow inclination.

The method of solution by the application of the above characteristic equations is similar in almost all respects to the ordinary methods developed for equilibrium flow except that in addition the rate of change of the n components of the gas along a streamline are to be determined by the n equations (27).

5. Reaction rates

The explicit forms of the terms ω_i which determine the rate of production of the various components of the gas have not yet been discussed. Since air is composed mainly of oxygen and nitrogen and it is assumed that other components have a negligible effect on the reaction rates for oxygen and nitrogen, only the dissociation and recombination rates of these two gases will be treated here. The following presentation is based on Logan's modification of simple collision theory and attempts to account approximately for the effects of the interaction of the internal degrees of freedom during the collision process.

Air is assumed to consist of oxygen and nitrogen atoms and molecules only. The process of dissociation, which involves collisions between a molecule and some other particle, is considered first. Since only simple molecules and atoms are present, the number of pairs of rotational degrees of freedom which are effective in transferring energy during the collision process is assumed to be one.

By considering the molecules in each vibrational state as a separate species, the energy required to dissociate a molecule in its nth vibrational state is then $D - E_n$, where D is the dissociation energy and E_n is the vibrational energy of the nth state. The rate of dissociation for a diatomic molecule considering all vibrational states is given by

$$\frac{d\nu}{dt} = -\sum_n Z_n \alpha_n \left(\frac{D-E_n}{kT}\right) \exp\left[-\left(\frac{D-E_n}{kT}\right)\right], \tag{31}$$

where ν is the number of particles per unit volume, and α_n represents the percentage of molecules in each vibrational state. From statistical mechanics, we have

$$\alpha_n = \alpha_0 \exp\left(-E_n/kT\right),$$

where α_0 is the percentage of molecules in the zeroth vibrational state. Z is the total number of collisions per unit volume and per unit time and is given by

$$Z = \frac{2\nu_1\nu_2}{\sigma_{12}} d_{12}^2 \left(\frac{2\pi kT}{\mu}\right)^{\frac{1}{2}},$$

where k is Boltzmann's constant, d_{12} is the average diameter and is the reduced mass of the colliding particles, and σ_{12} is a symmetry factor which is equal to one if the colliding particles are of different species and is equal to two if of the same

species. The subscript 1 refers to the molecules under consideration and the subscript 2 refers to all other colliding particles.

The additional assumption is made that all reaction partners are equally effective in causing dissociation. The rate of dissociation for the molecules m can then be written in the form

$$\frac{dv_m}{dt} = -k_d v_m \sum_i v_i, \tag{32}$$

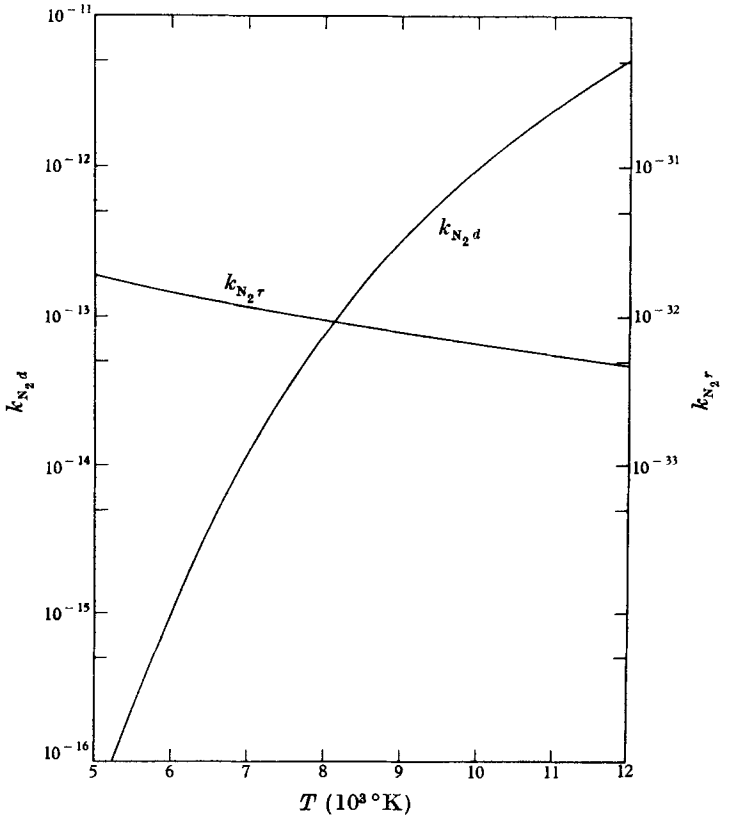

FIGURE 2. Dissociation and recombination rate constants for nitrogen.

where k_d is the dissociation rate constant and is a function of temperature only. The summation is to be taken over all particles i. By equating equations (31) and (32), k_d can be evaluated.

Similarly, for the case of recombination, which requires a three-body collision between two atoms a and another particle i, the rate can be written as

$$\frac{dv_m}{dt} = k_r v_a^2 \sum_i v_i. \tag{33}$$

The recombination rate constant k_r can now be evaluated using equilibrium theory. At equilibrium

$$\frac{dv_m}{dt} = k_r v_a^2 \sum_i v_i - k_d v_m \sum_i v_i = 0,$$

and therefore

$$\frac{k_d}{k_r} = \frac{\nu_a^2}{\nu_m} = K_e, \tag{34}$$

where K_e is the equilibrium constant and is a known function of temperature.

The dissociation and recombination rate constants were evaluated for both nitrogen and oxygen. The results are shown in figures 2 and 3. The variable ω_i is related to the above rate constants by

$$\omega_i = \frac{M_i}{N}\frac{d\nu_i}{dt},$$

where N is Avagadro's number.

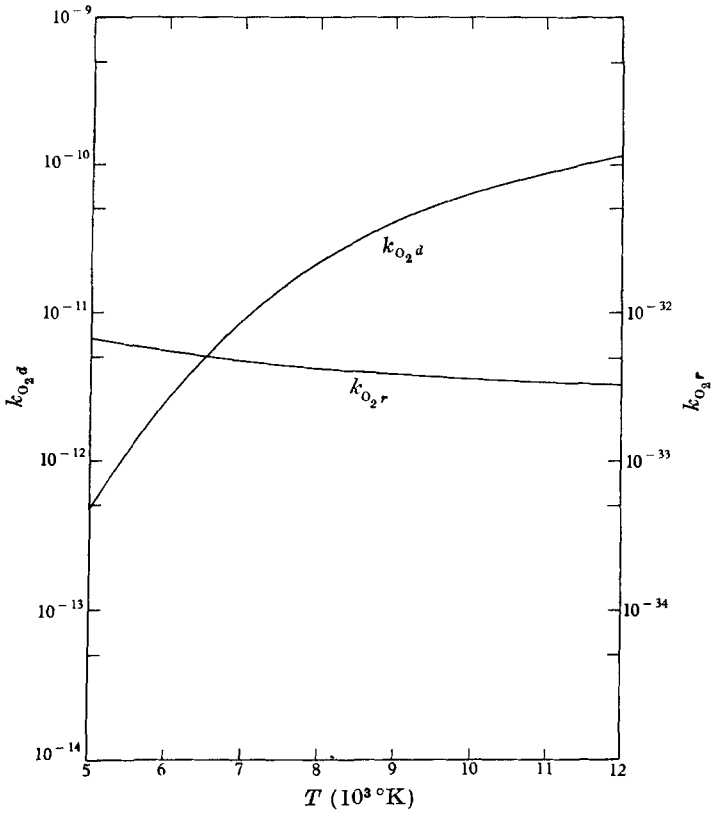

FIGURE 3. Dissociation and recombination rate constants for oxygen.

6. Numerical computations

By using the inverse method, the method of characteristics, and the previously determined dissociation and recombination rates, four numerical examples were calculated for the flow of a gas through a specified shock shape at a Mach number of 14 and for free-stream density and temperature corresponding to the density and temperature of air at an altitude of 100,000 ft. The calculation of the boundary conditions and the inverse method were programmed in floating point on the IBM 650. The flow conditions in the supersonic region calculated by the inverse

method were partially checked and slightly extended by hand computation using the method of characteristics.

The gas treated in the first three examples consisted of a mixture of oxygen and nitrogen in the same ratio to each other as in atmospheric air, an approximation to the real composition of air. To show the effects of non-equilibrium flow, various shock radii were chosen, so that a typical relaxation distance for oxygen dissociation near the stagnation streamline in comparison with the detachment distance was (i) small and the flow was practically in equilibrium throughout, (ii) of the same order of magnitude and the flow was only partially in equilibrium, and (iii) very large and no dissociation or recombination occurred.

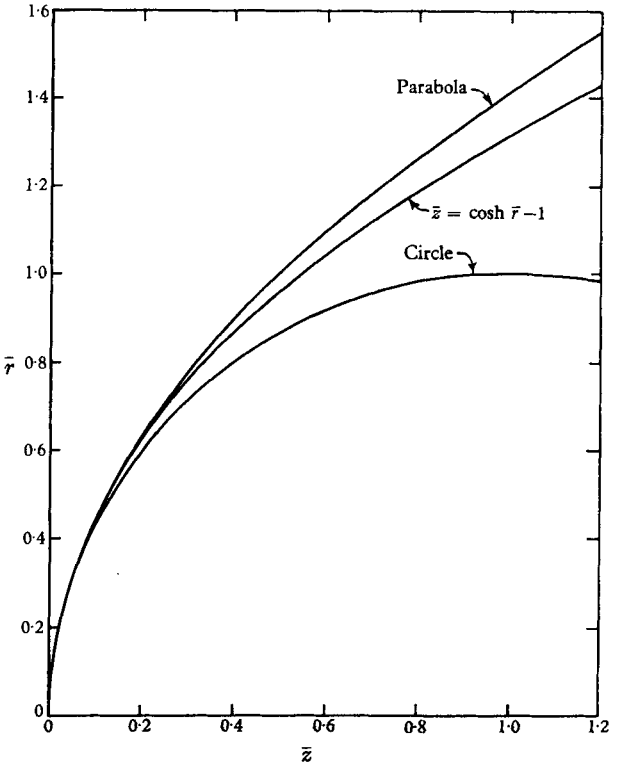

FIGURE 4. Shape of assumed shock.

To demonstrate also the effects of non-equilibrium flow on a pure gas, numerical results were obtained for the flow of pure oxygen for the case (ii) mentioned above.

To begin the computations, the shape of the shock must be specified. Preferably, the assumed shock shape must resemble closely the shocks produced by typical blunt-nosed bodies. For convenience in numerical computations, an analytic shock shape is desired wherein all shock variables dependent on the co-ordinate system such as $d\theta/dx$, $\sin\theta$, $\cos\theta$, and the position variables of the shock, r and z, can be expressed in terms of x, the co-ordinate parallel to the shock surface (see figure 1).

These properties are fulfilled by the curve known as the catenary, which is compared with the parabola and circle in figure 4 and which is given by

$$\bar{z} = \cosh \bar{r} - 1, \tag{36}$$

where the bars denote quantities made non-dimensional with respect to R_0, the radius of curvature of the shock on the axis of symmetry. Of course, the co-ordinate system can be adapted to an almost completely arbitrary shock shape as produced by blunt-nosed bodies including shock shapes with inflexion points.

By using the iteration procedure described previously, the conditions at the shock were calculated at 50 values of $\bar{x}$ at equally spaced intervals $\Delta\bar{x} = 0{\cdot}04$ starting at $\bar{x} = 0{\cdot}02$ in order to avoid, in later computations, the indeterminate forms $(u/r)\,(\partial r/\partial x)$ and $(v/r)\,(\partial r/\partial y)$ at $\bar{x} = 0$. After the boundary conditions at the shock have been found, the solution can be continued in the subsonic and slightly supersonic regions by the inverse method and in the supersonic region by the method of characteristics. In these computations, it was found convenient to write the governing equations in terms of the dimensionless quantities

$$\bar{V} = \frac{V}{V_\infty}, \quad \bar{P} = \frac{P}{\rho_\infty V_\infty^2}, \quad \bar{\rho} = \frac{\rho}{\rho_\infty}, \quad \bar{T} = \frac{T}{T_\infty}.$$

7. Results and discussion

In the three problems calculated for air, the free-stream conditions and the shock shape are identical, and therefore the shock boundary conditions are also identical. The differences in the flow quantities in the field are then dependent on a local non-equilibrium parameter χ, which can be shown from the non-dimensional equations to be $(R_0/\rho_\infty V_\infty)\,(\omega_{O_2}/\bar{\rho})$ or $(R_0/\rho_\infty V_\infty)\,(\omega_{N_2}/\bar{\rho})$. The parameter R_0/V_∞ is a characteristic time associated with the flow, while either $(\omega_{O_2}/\rho_\infty\bar{\rho})^{-1}$ or $(\omega_{N_2}/\rho_\infty\bar{\rho})^{-1}$ is a characteristic time associated with the non-equilibrium process. χ_{O_2}, evaluated at $x = y = 0$, was chosen to vary over a range from practically equilibrium flow ($\chi_{O_2} = 100$, $R_0 = 10$ cm) through partial equilibrium flow ($\chi_{O_2} = 5$, $R_0 = 0{\cdot}5$ cm) to frozen dissociation flow ($\chi_{O_2} = \chi_{N_2} = 0$).

From the results of the computations, two regions of the flow field were found to be of particular interest: (1) the region near the axis of symmetry, where the flow behaves similarly to the flow through a normal shock and where the finite dissociation rates have a large influence on the flow properties, and (2) the region of flow expansion around the body near the surface, where the finite recombination rates have a large influence on the flow properties. The variations of α_0, $\bar{V}$, $\bar{p}$, $\bar{\rho}$, and $\bar{T}$ in these two regions for the three examples calculated for air are shown in figures 5 to 14. The variation of α_N for air is not given since in the present problems the dissociation of nitrogen is negligibly small.

Figure 5 presents the distribution of oxygen atoms along the stagnation streamline for $\chi_{O_2} = 100$ and $\chi_{O_2} = 5$. For $\chi = 0$, since the dissociation rate is zero, α_0 is constant and equal to zero throughout the shock layer. It can be seen that for $\chi_{O_2} = 100$, the oxygen dissociation is near equilibrium a short distance from the shock, while for $\chi_{O_2} = 5$, the dissociation is not in equilibrium until the stagnation point is reached. Both cases show the rapid dissociation near the shock due to the high temperatures and the exponential factor in the dissociation rate.

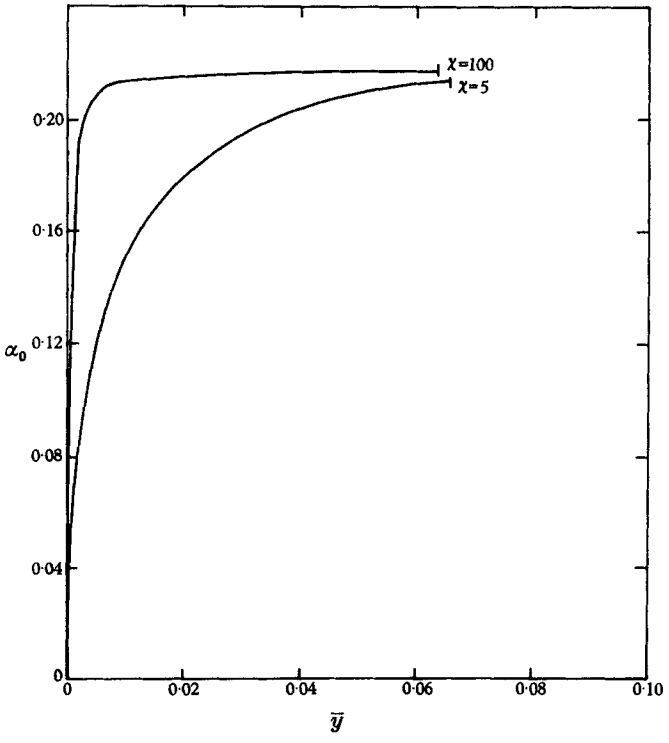

FIGURE 5. Variation of mass fraction of atomic oxygen α_0 along the stagnation streamline.

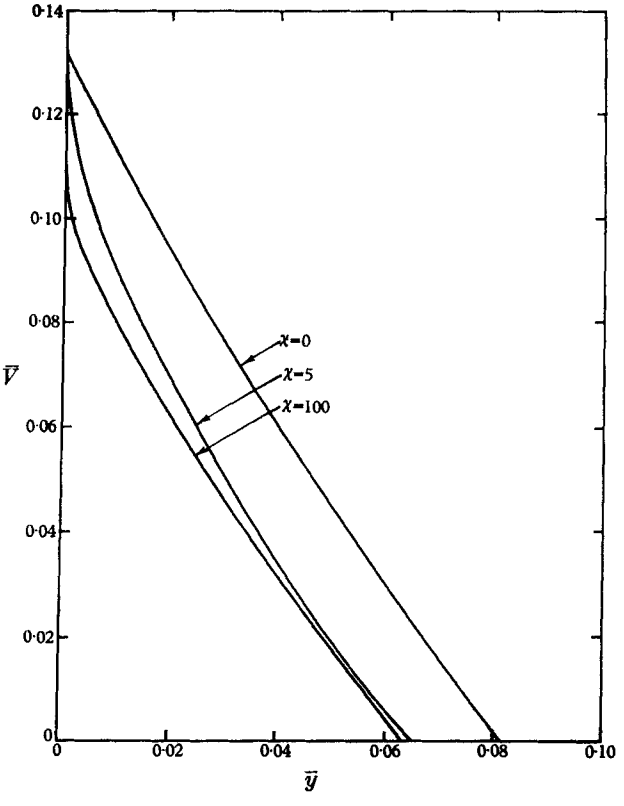

FIGURE 6. Variation of velocity $\bar{V}$ along the stagnation streamline.

The effect of the non-equilibrium is evident in figure 6 showing the variation of $\overline{V}$ along the stagnation streamline. For $\chi_{O_2} = 100$, dissociation causes a rapid decrease in $\overline{V}$ near the shock. The detachment distance can be seen to be approximately 0·064.* For $\chi_{O_2} = 5$, the decrease in the velocity is less abrupt. The detachment distance has increased to approximately 0·066. For $\chi = 0$, little change in gradient of the velocity occurs. The shock detachment distance is approximately 0·081.

The effect of the dissociation on the pressure, density, and temperature is similar to the effect on the velocity as can be seen from figures 7 to 9. Large variations in the flow quantities occur near the shock for $\chi_{O_2} = 100$. For $\chi_{O_2} = 5$, the variations are less rapid but extend to the stagnation point. For $\chi = 0$, the changes in $\overline{p}$, $\overline{\rho}$, and $\overline{T}$ are comparatively very small.

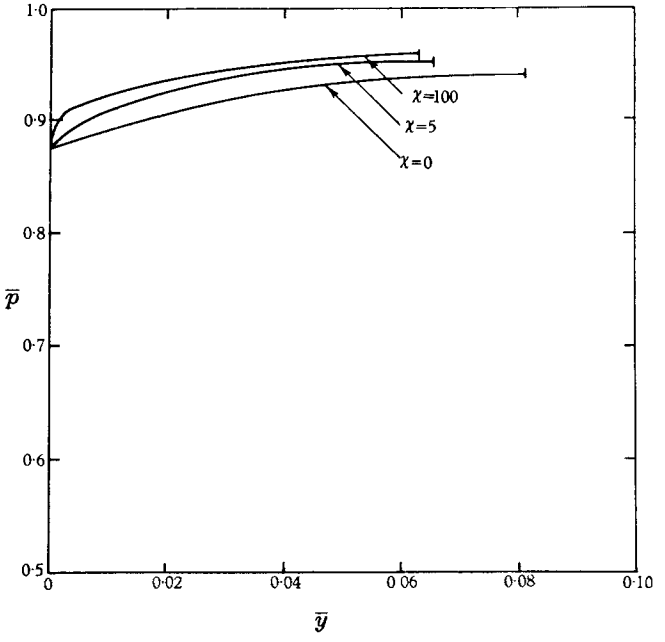

FIGURE 7. Variation of pressure $\overline{p}$ along the stagnation streamline.

Finite reaction rates have little effect on pressure as can be expected from normal shock-wave theory. However, dissociation causes the density to increase greatly, which is the main reason for the decrease in detachment distance as χ increases. The most dramatic effect of dissociation is the temperature drop near the shock due to the absorption of energy by the dissociating molecules offsetting the slight increase in temperature due to compression of the gas near the stagnation point.

* Note that all distances are made non-dimensional with respect to R_0, the radius of curvature of the shock at $\overline{x} = 0$. For detachment distances made non-dimensional with respect to the radius of curvature of the body at $\overline{x} = 0$, the detachment distances as presented here must be multiplied by the ratio of the shock radius of curvature to the body radius of curvature, approximately 1·3 in the present case.

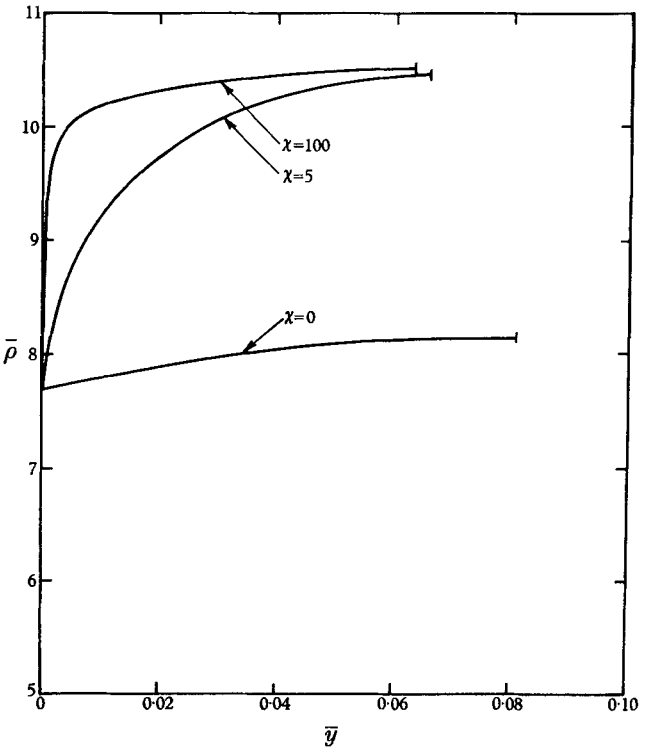

FIGURE 8. Variation of density $\bar{\rho}$ along the stagnation streamline.

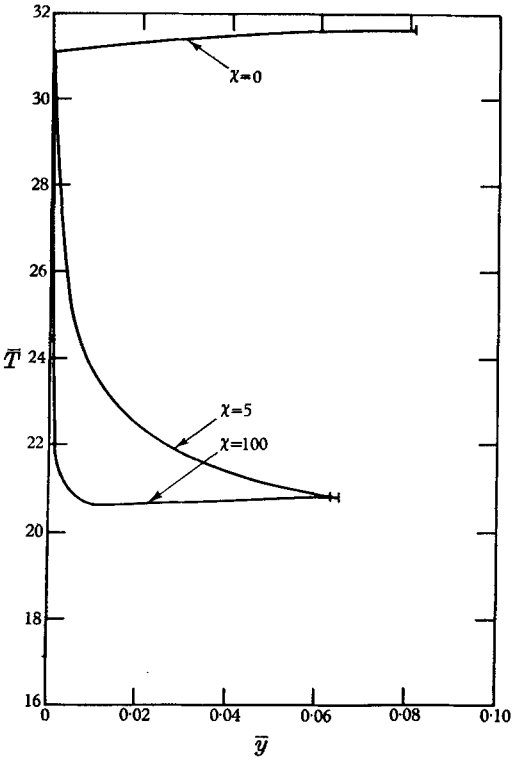

FIGURE 9. Variation of temperature $\bar{T}$ along the stagnation streamline.

The variation of α_0 along the body surface is shown in figure 10. It can be seen that the percentage of oxygen dissociated is slightly higher near the stagnation point for $\chi_{O_2} = 100$ than for $\chi_{O_2} = 5$. However, as $\bar{x}$ increases, the amount of oxygen dissociated soon becomes greater for $\chi_{O_2} = 5$, indicating that the flow is partially frozen as it expands along the body surface.

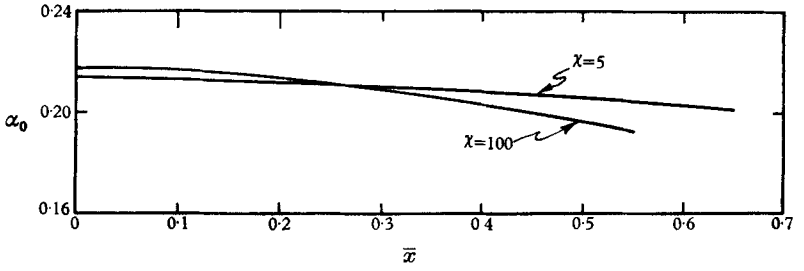

FIGURE 10. Variation of mass fraction of atomic oxygen α_0 along surface of body.

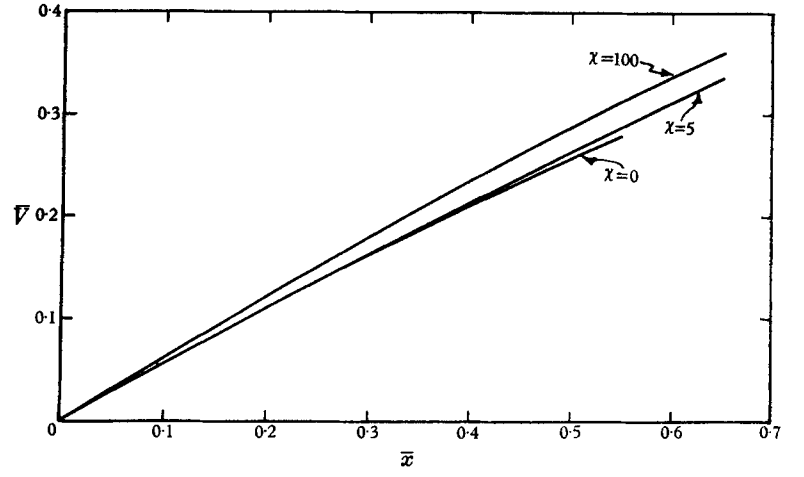

FIGURE 11. Variation of velocity $\bar{V}$ along surface of body.

The effect of the finite recombination rates on $\bar{V}$, $\bar{p}$, $\bar{\rho}$ and $\bar{T}$ on the body surface are shown in figures 11 to 14. There is little effect on the velocity except in the limiting case of frozen flow. It can be seen from figure 12 that, although the pressure at the stagnation point is different for all three bodies, the rate of decrease from this maximum is almost identical. For purposes of comparison, the Newtonian pressure is shown for the case $\chi_{O_2} = 100$. It can be shown that the effect of the non-equilibrium flow is to slightly increase the disagreement between the calculated and Newtonian pressure.

The finite recombination rate causes the density to fall off less rapidly as the gas expands, as can be seen from figure 13. The large differences in temperatures on the three bodies due to dissociation and recombination is shown in figure 14. Also noticeable is the greater rate of decrease in temperature for $\chi_{O_2} = 5$ and $\chi = 0$ due to the fact that in a rapidly expanding flow the recombination rate may be less than necessary to keep the flow in equilibrium. In this circumstance, the inert

degrees of freedom will retain their energy, and the temperature of the active degrees of freedom must decrease more rapidly to compensate for this.

For the fourth calculation, that of pure oxygen, the same shock shape was assumed. Although the free-stream density and temperature were chosen

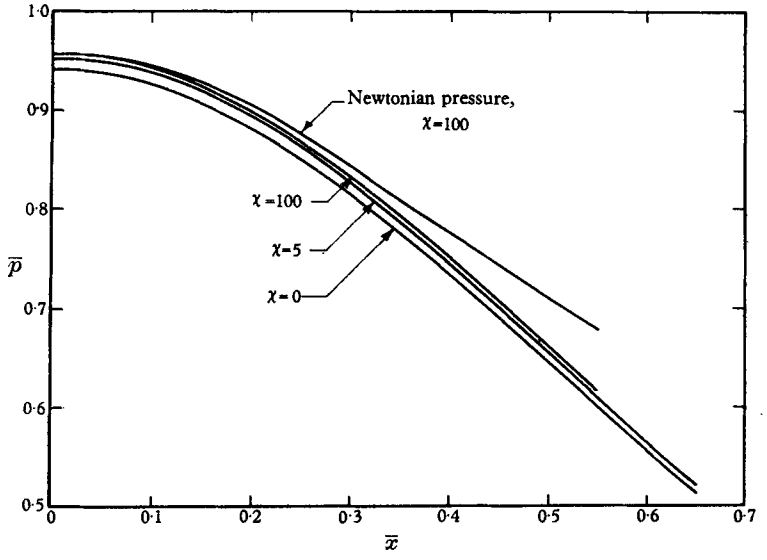

FIGURE 12. Variation of pressure $\bar{p}$ along surface of body.

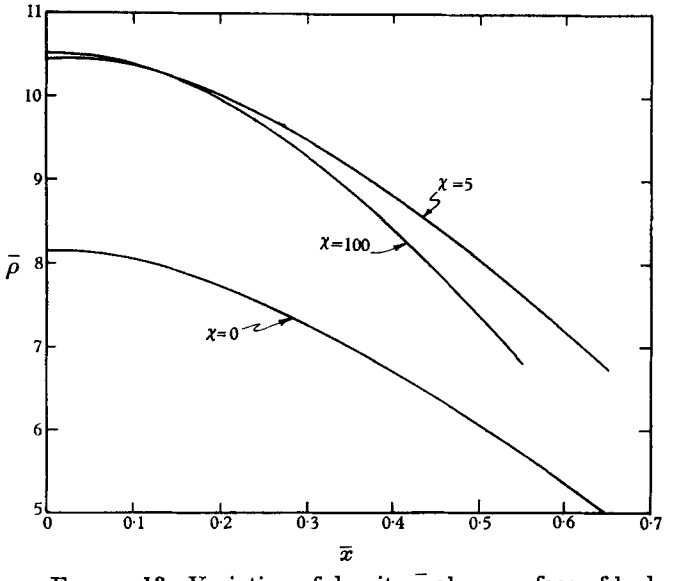

FIGURE 13. Variation of density $\bar{\rho}$ along surface of body.

identical with those in the previous examples, the free-stream pressure was not the same due to a change in the molecular weight of the gas. Therefore the shock boundary conditions were not the same as before. A greater amount of the gas is dissociated in this case than in the previous examples. A correspondingly greater effect on the flow field is expected and does result. Except that the variations are

greater than for air with $\chi_{O_2} = 5$, the shape of the curves and general appearance of the flow fields are similar.

A limitation to the present computational results is the inadequate knowledge of dissociation and recombination rates. A variation in the actual reaction rates from those assumed here of course does not invalidate the present results but does make the results applicable to bodies of different size. Another limitation to the

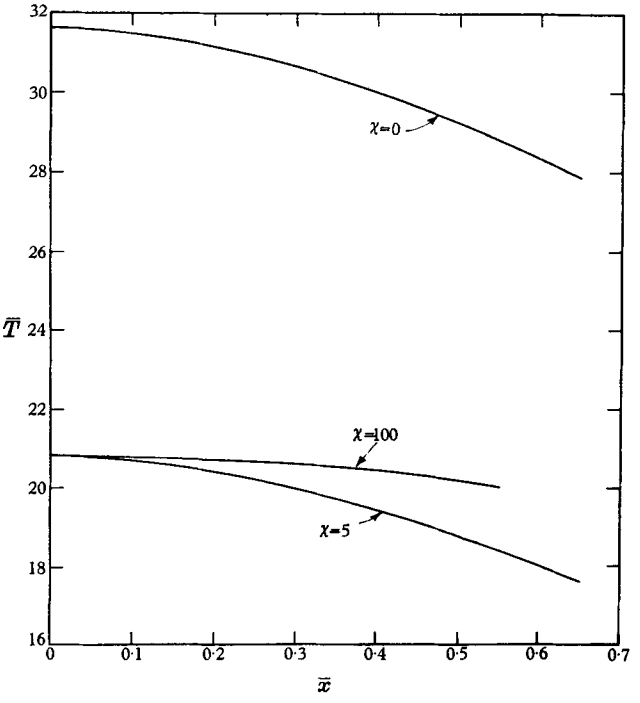

FIGURE 14. Variation of temperature $\bar{T}$ along surface of body.

present results for air is the assumption that air consists of a mixture of oxygen and nitrogen atoms and molecules. No account has been taken of the interaction of oxygen and nitrogen with each other to form NO or other compounds, which may have an effect on the gas properties and especially the reaction rates.

REFERENCES

FREEMAN, N. C. 1957 Dynamics of a dissociating gas. III. Non-equilibrium theory. *NATO Rep.* no. 133.

GUNN, J. C. 1952 Relaxation time effects in gas dynamics, R and M. *A.R.C. Tech. Rep.* no. 2338.

HIRSCHFELDER, J. O., CURTISS, C. F. & BIRD, R. B. 1954 *Molecular Theory of Gases and Liquids.* New York: Wiley.

LOGAN, J. 1957 Relaxation phenomena in hypersonic aerodynamics. *I.A.S. Preprint,* no. 728.

PENNER, S. S. 1955 Chemical reactions in flow systems. *AGARD Rep.* no. 7.

VAN DYKE, M. 1958 The supersonic blunt-body problem—review and extension. *I.A.S. Preprint,* no. 801.

ZLOTNICK & NEWMAN 1957 Theoretical calculation of the flow on blunt-nosed axisymmetrical bodies in a hypersonic stream. *AVCO TR-2-57-29.*